ELSEVIER

Earth and Planetary Science Letters 202 (2002) 61–75

EPSL

www.elsevier.com/locate/epsl

African monsoon variability during the previous interglacial maximum

E.J. Rohling [a,*], T.R. Cane [b], S. Cooke [a], M. Sprovieri [c], I. Bouloubassi [d], K.C. Emeis [e], R. Schiebel [f], D. Kroon [g], F.J. Jorissen [h], A. Lorre [d], A.E.S. Kemp [a]

[a] *University of Southampton, School of Ocean and Earth Science, Southampton Oceanography Centre, Waterfront Campus, European Way, Southampton, Hampshire SO14 3ZH, UK*
[b] *School of Chemistry, Physics and Environmental Science, University of Sussex, Falmer, Brighton BN1 9QJ, UK*
[c] *Dipartimento C.F.T.A., University of Palermo, Via Archirafi, 36 90123 Palermo, Italy*
[d] *Laboratoire de Physique et Chimie Marines, Université Pierre et Marie Curie, 4 place Jussieu, 75252 Paris Cedex 05, France*
[e] *Institut für Ostseeforschung Warnemünde, Seestrasse 15, D-18119 Warnemünde, Germany*
[f] *Geological Institute, Eidgenössische Technische Hochschüle Zürich, Sonneggstrasse 5, NOG 32.2, 8092 Zürich, Switzerland*
[g] *Faculty of Earth Sciences, De Boelelaan 1085, 1081 HV Amsterdam, The Netherlands*
[h] *Laboratoire de Géologie, Faculté Sciences, Université d'Angers, 2 Boulevard Lavoisier, 49045 Angers Cedex, France*

Received 11 February 2002; received in revised form 17 June 2002; accepted 17 June 2002

Abstract

Little is known about centennial- to millennial-scale climate variability during interglacial times, other than the Holocene. We here present high-resolution evidence from anoxic (unbioturbated) sediments in the eastern Mediterranean Sea that demonstrates a sustained ~800-yr climate disturbance in the monsoonal latitudes during the Eemian interglacial maximum (~125 ka BP). Results imply that before and after this event, the Intertropical Convergence Zone (ITCZ) penetrated sufficiently beyond the central Saharan watershed (~21°N) during the summer monsoon to fuel flooding into the Mediterranean along the wider North African margin, through fossil river/wadi systems that to date have been considered only within a Holocene context. Relaxation in the ITCZ penetration during the intra-Eemian event curtailed this flux, but flow from the Nile – with its vast catchment area – was not affected. Previous work suggests a concomitant Eurasian cooling event, with intensified impact of the higher-latitude climate on the Mediterranean basin. The combined signals are very similar to those described for the Holocene cooling event around 8 ka BP. The apparent type of concurrent changes in the monsoon and higher-latitude climate may reflect a fundamental mechanism for variability in the transfer of energy (latent heat) between the tropics and higher latitudes.

Keywords: Eemian; Mediterranean region; sapropel; monsoons

1. Introduction

It has become well established that global climate fluctuated on centennial to millennial time

* Corresponding author. Tel.: +44-1703-593042; Fax: +44-1703-593059.
E-mail address: e.rohling@soc.soton.ac.uk (E.J. Rohling).

0012-821X/02/$ – see front matter
PII: S0012-821X(02)00775-6

scales between remarkable extremes during the last glacial cycle (75–11.5 ka BP) [1–8], and that similarly timed but lower-amplitude fluctuations continued during the present interglacial period (Holocene: 11.5 ka BP to Present) [2,9–12]. To understand the potential impact of natural climate variability on a greenhouse future, a detailed study has been undertaken of the previous interglacial maximum – Marine Isotope Stage (MIS) 5e (Eemian) – when sea level stood ~6 m above the present [13,14] and global temperatures were ~2°C higher than today [15,16]. The Eemian coincided with a particularly strong northern summer insolation maximum, driven by the coincidence of a minimum in the 21-kyr astronomical cycle of precession with a distinct maximum in orbital eccentricity, which greatly enhanced the intensity of moisture-bringing summer monsoon circulation on the northern hemisphere [17–19]. Initial reports from Greenland ice records of intensive centennial- to millennial-scale Eemian climate variability are now held to be uncertain due to ice-flow distortions prior to ~110 ka BP [20]. With ice cores being unable to provide a 'template' of climate variability for the Eemian such as that available for the last 110 kyr, there is a specific need for unbioturbated lacustrine and marine sediment records of the Eemian from climatically sensitive settings.

The eastern Mediterranean offers an excellent target for such an investigation of the Eemian, because: (1) the basin critically resides at the boundary between the subtropical and mid/high latitude climate systems, and therefore is highly sensitive to even subtle reorganisations; (2) sediment accumulation rates in this land-locked basin are commonly higher than in the open oceans; (3) the basin's relatively small volume specifies a lack of inertia, so that its properties respond rapidly and in an amplified fashion (high signal-to-noise ratio) to climatic perturbations; and (4) the Eemian is marked in the eastern Mediterranean by a phase of anoxic (sapropel) sedimentation, which precluded benthic life and consequently bioturbation, thereby preserving undisturbed highly-resolved records. The Eemian interval of anoxic sediments in the eastern Mediterranean is named sapropel S5, with an estimated duration of 3–6 kyr [21], in close agreement with the ^{230}Th–U age range of 124–119 ka BP for the Eemian peak wet phase in Soreq Cave, Israel [22].

We here report data from three S5 sapropels (Fig. 1), found at 482.5–506.0 cm in piston core KS205, 40.2–63.0 cm in ODP Site 971A section 1H-3, and 74.5–103 cm in ODP Site 967C section 1H-5 [21]. Using a 5-kyr duration [22], the average sediment accumulation rates through these S5 sapropels are 4.7, 4.6, and 5.7 cm kyr^{-1}, respectively. First, the basic approach and the crucial aspects of the stratigraphic framework for the investigated S5 records are discussed. Next, the results are captured in a main working hypothesis of Eemian monsoon variability. After a critical evaluation against two potential counter hypotheses (which are rejected), the inferred Eemian variability is considered within a wider regional and temporal context of climate variability throughout the Eemian, last glacial cycle, and Holocene. The concluding remarks address the importance of the reconstructed type of monsoon fluctuations for validation of possible climate responses to solar variability, and express the need for improved understanding of the linkage between low- and high-latitude climate variability on centennial to millennial time scales.

2. Methods

The data set for S5 in the three sites discussed here comprises planktonic foraminiferal abundance records and stable oxygen and carbon isotope records for the planktonic foraminiferal species *Globigerinoides ruber* (white), *Neogloboquadrina pachyderma* (dextral) and *Globorotalia scitula*. In the case of core KS205, we have furthermore analysed the isotope records of large-diameter spherical *Orbulina universa* and wide open-coiled *Globigerinella siphonifera*. All analyses were performed with a Europa Geo2020 mass spectrometer following reaction, in individual acid baths, of 3–10 handpicked and cleaned adult specimens within a 50–100-μm size window. Isotope ratios are expressed as $\delta^{13}C$ and $\delta^{18}O$, in ‰ values relative to Vienna PeeDee Belemnite,

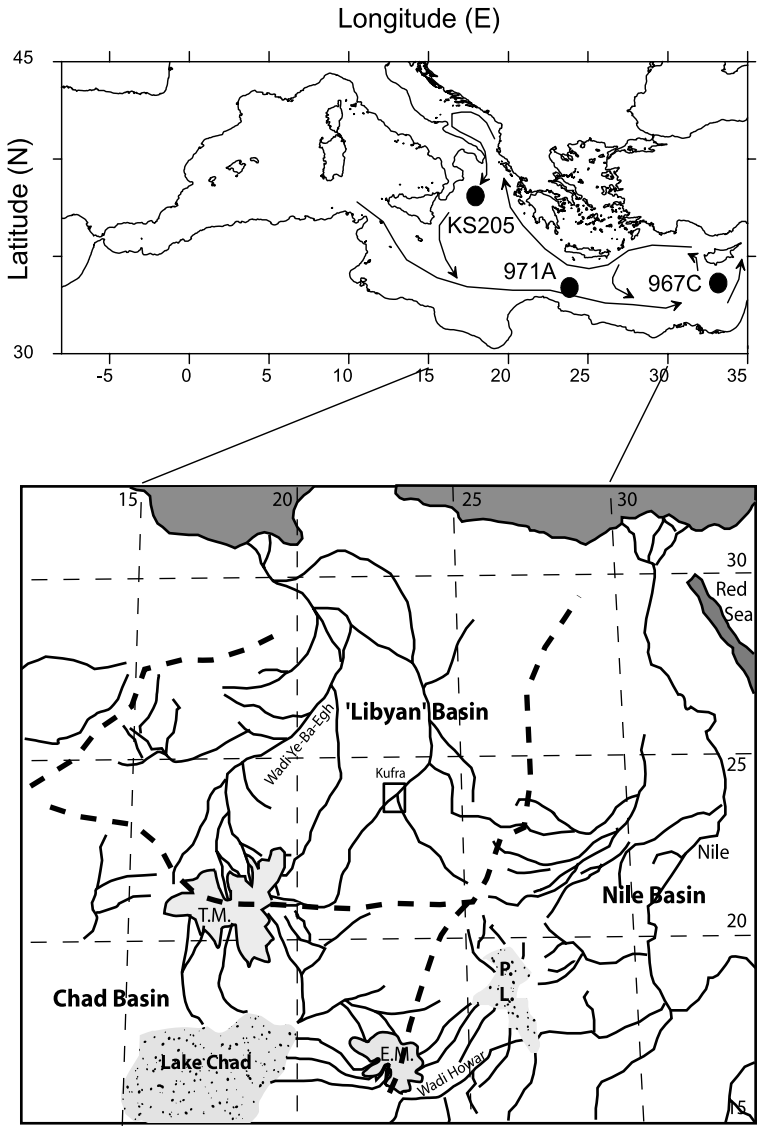

Fig. 1. Map of the Mediterranean with core locations and schematic generalisation of present-day surface circulation patterns. The expanded map of the Libyan–Egyptian sector of North Africa with river/wadi systems noted for the Holocene monsoon maximum (after a much more detailed map in [45]), shows rough positions of the main watersheds separating the Nile Basin, Chad Basin, and 'Libyan Basin' (heavy dashed lines, after [47,48]). Box marked Kufra gives approximate site of the cited Space-shuttle radar image [46]. Abbreviations: T.M., Tibesti Mountains; E.M., Ennedi Mountains; L.P., Lake Ptolomy [45].

and external precision was better than 0.06‰ for both $\delta^{13}C$ and $\delta^{18}O$.

We also obtained century-scale resolution Sea Surface Temperature (SST) records based on the alkenone unsaturation index $U^{k'}_{37} = C_{37:2}/(C_{37:2}+C_{37:3})$. Sediments were solvent extracted by ultrasonication (core KS205, Hole 967C) or in a Dionex ASE 200 Accelerated Solvent Extractor (Hole 971A). Alkenone fractions were isolated by silica gel column chromatography (core KS205) or by high pressure liquid chromatography (Hole 967C), and analysed by capillary gas chromatography. Detailed procedures have been reported elsewhere [23] or are available on request

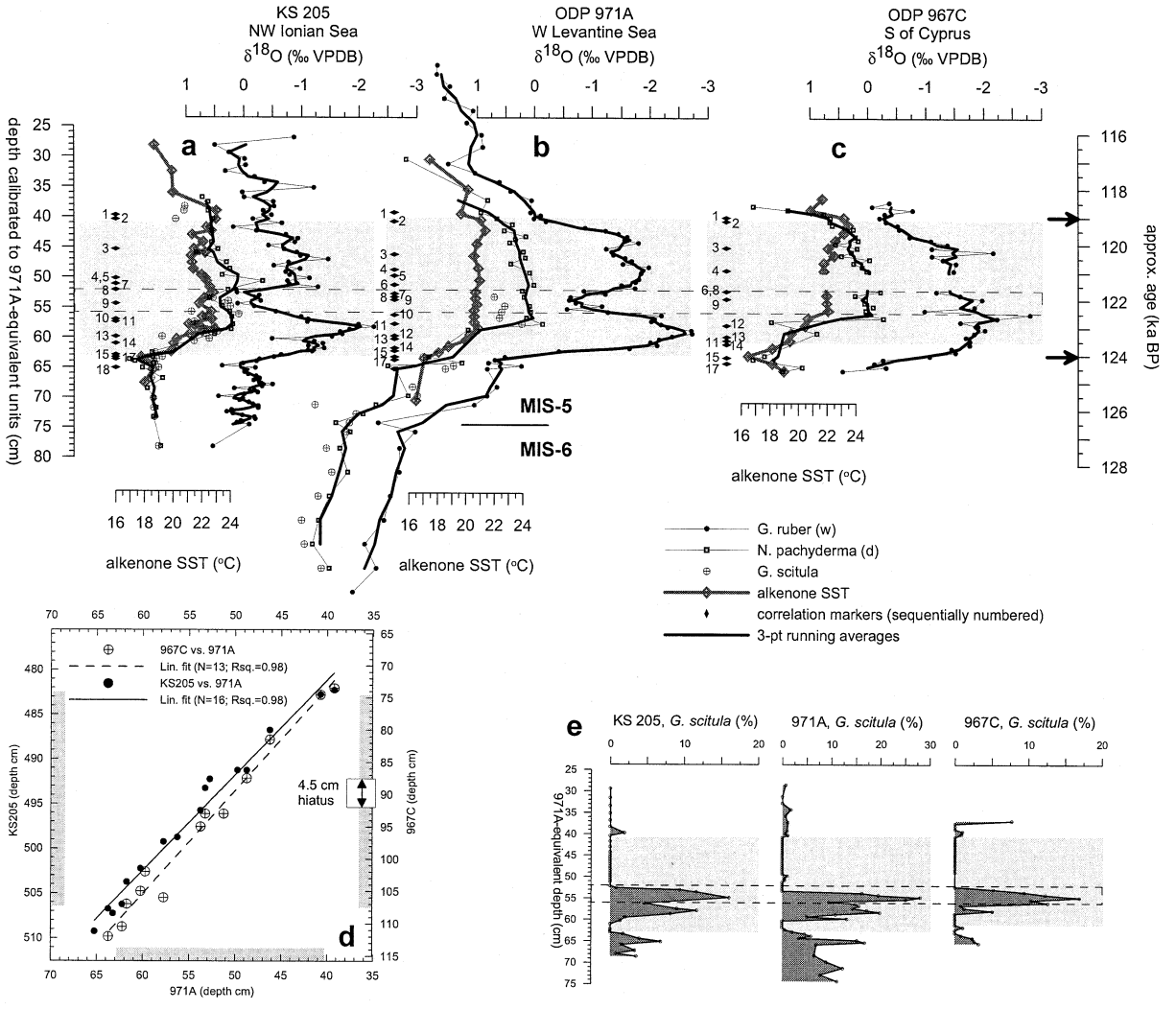

Fig. 2. (a–c) Stable oxygen isotope records for the planktonic foraminiferal species *G. ruber* (w), *N. pachyderma* (d), and *G. scitula* through Eemian sapropel S5 in core KS205 (38°11.86′N; 18°08.04′E; 2384 m), and ODP sites 971A (24°41′N; 33°43′E; 2026 m) and 967C (34°04.27′N; 32°43.53′E; 2554 m), all plotted versus the 971A-equivalent depth scale based on the calibrations of [21]. Numbered markers represent primary correlation levels between the sites [21], sequentially numbered here from top to base. Grey blocks indicate the visual extent of the dark-coloured sapropel sediments in each core, the bases of which correspond to benthic extinction levels that indicate the development of persistent sea-floor anoxia [21]. Dashed block highlights the interval containing the discussed $\delta^{18}O_{G.\ ruber\ (w)}$ anomaly in KS205 and 971A. The approximate time scale given is based on simple linear interpolation through the ages of 124 and 119 ka BP (arrows) for the onset and end of the humid phase coincident with S5 deposition [22]. (d) Representation of the highly significant linear regressions used to calibrate KS205 and 967C to 971A-equivalent depth (after [21]). Grey bars again indicate visual extent of dark-coloured sapropel sediments, which was *not* used in the correlation exercise to avoid bias by diagenetic change to sediment colour. The 4.5-cm gap in 967C [21] postdates the interval with the return to heavier $\delta^{18}O_{G.\ ruber\ (w)}$ values in the two western sites. (e) Abundance records of *G. scitula* illustrating the distinct abundance peak, followed by an abrupt drop to total absence, within the dashed block that marks the interval containing the $\delta^{18}O_{G.\ ruber\ (w)}$ anomaly in KS205 and 971A (see panels a–c).

[acknowledgements]. The methodologies used in the two analytical facilities involved (Warnemünde and Paris) have been intercalibrated [24]. The $U^{k'}_{37}$ index was translated into temperatures using the global calibration [25]: SST (°C) = ($U^{k'}_{37}$ − 0.044)/0.033. Previous work [26,27] elaborated why this equation should be favoured for annual average temperature reconstructions, relative to the (seasonal) relationship from western Mediterranean sediment-trap data [28].

Using the independent SST data, it is possible to deduce the magnitude of temperature-related change in the isotope records, thus isolating the residual signals. Since ice-volume effects on the isotope records were weak during the Eemian high stand, and would be of equal timing and magnitude in all records for all species at all sites, the residual signals are viewed in terms of processes involving the freshwater balance within the basin.

3. Stratigraphic framework

Three Eemian sections on a West–East transect through the eastern Mediterranean (Fig. 1) were sampled and analysed in sub-century resolution (Fig. 2). In a recent stratigraphic study [21], the three sections were correlated with one another through statistical comparisons between strong (multi-sample) O and C isotope shifts and clear faunal presence/absence levels. Positions of the primary correlation markers used in that regression exercise are indicated with sequential numbering in Fig. 2a–c.

The stratigraphic study [21] developed regressions to calibrate the KS205 and 967C depth scales to 971A-equivalent depths (summarised in Fig. 2d). The procedure involved a least squares fit through an unweighted cloud of primary correlation markers, to identify the best calibration between the depth-series, while allowing for potential diachroneity or uncertainty in each point (i.e. deviation of individual points from the regression line). No strict 'tie-points' were imposed, since no a priori assumptions were made as to the syn-/diachroneity of any of the correlation markers. To eliminate the possibility that a whole record could systematically lag another record if any single proxy were considered, correlation markers were used from three independent proxies. If all points were synchronous events and could be unambiguously placed in each record, then the regressions would come out with R^2 values of 1.0. In fact, the regressions came out with R^2 values very close to that (0.98), and the typical deviation of individual points from the regression lines was within ±1 cm. The high similarity in sequence and spacing of the events/markers from different independent proxies could only be explained in terms of (virtually) synchronous developments within the relatively small eastern Mediterranean basin.

Based on the regressions, the three records were calibrated to a common depth scale (that of S5 in ODP Hole 971A section 1H-3), to allow direct comparison of spatial and temporal gradients [21]. Plots of the main data against the common depth scale show a high degree of consistency in the signal structures between the three sites, which further corroborates the stratigraphic framework (Fig. 3). One of the most striking examples of a virtually synchronous event to appear from the framework is the abrupt and complete disappearance of the planktonic foraminifer *Globorotalia scitula* around 52–53 cm, immediately after an interval with high abundances at all three sites (Figs. 2 and 3). None of the records shows trace abundances of *G. scitula* for at least five samples (2.5 cm, ∼400 yr) after the event. The framework's suggestion that the disappearance of *G. scitula* was synchronous agrees with the common-sense argument that such an abrupt drop to sustained and absolute zero within the relatively small eastern Mediterranean ought to reflect a (virtually) synchronous species eradication from the entire basin: if it were diachronous, then sites affected first would show some continuation of (advected) trace abundances until the event had progressed throughout the basin.

The framework is refined enough to identify a minor (∼4.5 cm) gap/condensed interval in the S5 record of ODP Hole 967C (Figs. 2 and 3), in a position close to, but definitely postdating, the interval focussed on in the present paper. This sedimentary anomaly was obvious as a distinct

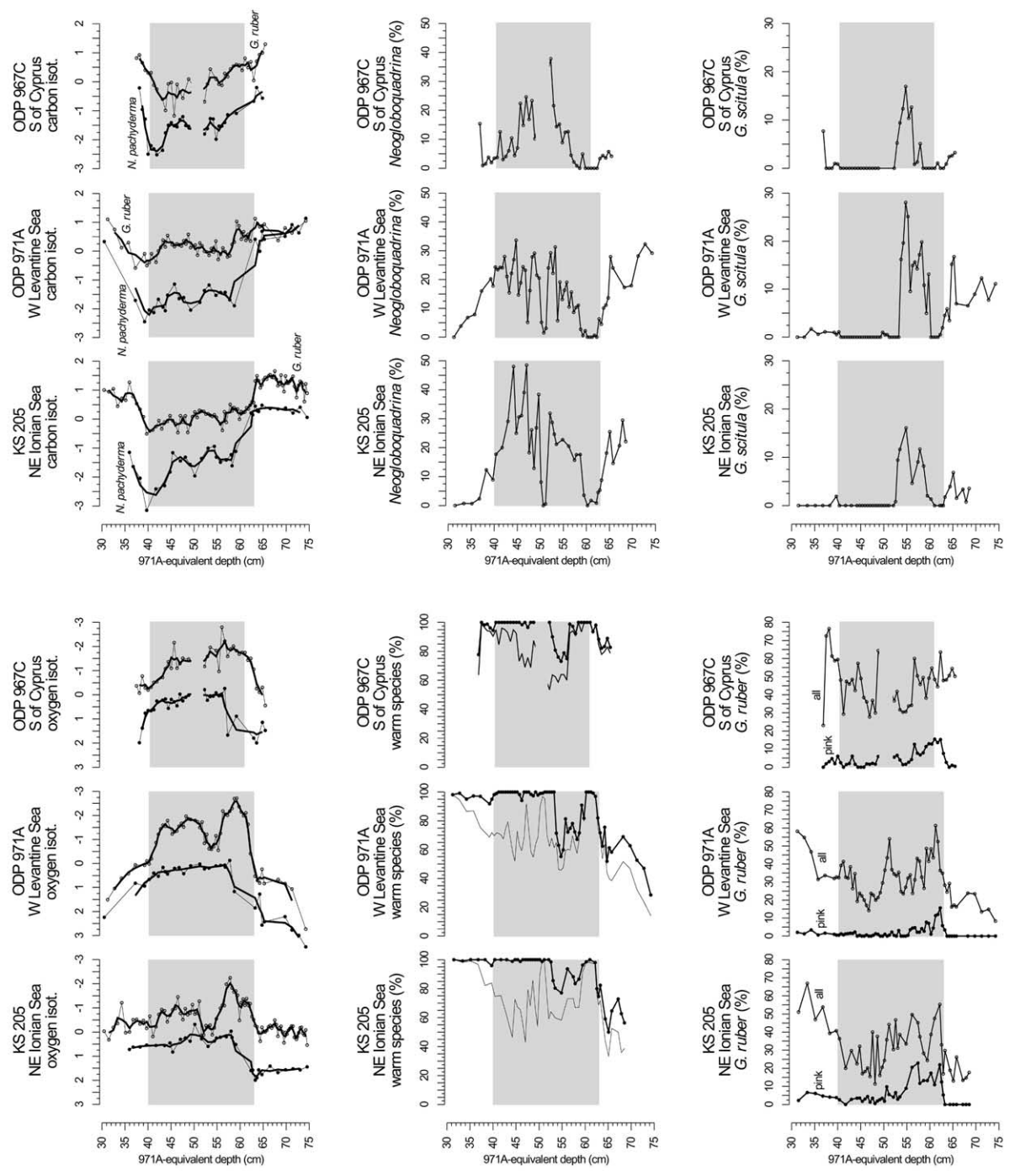
ODP 967C
S of Cyprus
carbon isot.
ODP 971A
W Levantine Sea
carbon isot.
KS 205
NE Ionian Sea
carbon isot.
N. pachyderma
G. ruber
ODP 967C
S of Cyprus
Neogloboquadrina (%)
ODP 971A
W Levantine Sea
Neogloboquadrina (%)
KS 205
NE Ionian Sea
Neogloboquadrina (%)
ODP 967C
S of Cyprus
G. scitula (%)
ODP 971A
W Levantine Sea
G. scitula (%)
KS 205
NE Ionian Sea
G. scitula (%)
ODP 967C
S of Cyprus
oxygen isot.
ODP 971A
W Levantine Sea
oxygen isot.
KS 205
NE Ionian Sea
oxygen isot.
ODP 967C
S of Cyprus
warm species (%)
ODP 971A
W Levantine Sea
warm species (%)
KS 205
NE Ionian Sea
warm species (%)
ODP 967C
S of Cyprus
G. ruber (%)
ODP 971A
W Levantine Sea
G. ruber (%)
KS 205
NE Ionian Sea
G. ruber (%)
all
pink
971A-equivalent depth (cm)

'platform' in the cross-plot of primary markers between the records for Holes 971A and 967C, separating two linear regressions of similar slope (slope above: 1.47 with $N = 5$ and $R^2 = 0.98$; slope below: 1.67 with $N = 8$ and $R^2 = 0.90$, respectively). After correction for the anomaly/gap in 967C responsible for the 'platform' of correlation markers, a highly significant regression with a similar slope (1.60; $N = 13$ and $R^2 = 0.98$), was obtained through the entire set of correlation markers, corroborating that the two separate regressions above and below the 'platform' were partial representations of a single underlying correlation regression [21].

In short, the multi-proxy character of the correlated data, the robustness of the regressions, and the validation by agreements in the general signal structure, imply that distinct lateral alignments represent (near) synchronous events between the three sites, within a ±1-cm confidence margin (roughly ±150–200 yr).

4. Results and discussion

4.1. Working hypothesis: Eemian monsoon variability

We here concentrate primarily on the alkenone SST records in combination with the $\delta^{18}O$ records for the planktonic foraminifera *G. ruber* (w), *N. pachyderma* (d) and *G. scitula* (Fig. 2). Being a well-known shallow (< 50 m) dwelling species with a peak abundance in late summer in the Mediterranean today [29], *G. ruber* (w) is appropriate for a characterisation of property changes due to the peak monsoon flooding (late summer). In contrast, *N. pachyderma* (d) and *G. scitula* thrive at depth (70–200 m) [29,30] and so reflect longer-term integrated records of change in the overall basin state, rather than high-frequency and surface-limited regional variability in the climatic forcing functions.

Fig. 2a–c show the SST fluctuations on a scale that is calibrated relative to the $\delta^{18}O$ axes so that every 1°C change in temperature corresponds to 0.23‰ in $\delta^{18}O$ [31,32]. The isotopic shifts in *N. pachyderma* (d) and *G. scitula* to a great extent reflect the record of SST change. The $\delta^{18}O$ records for *G. ruber* (w) on the contrary show much greater amplitudes of change, with the lightest values noted for the sapropel. Core KS205 and Hole 971A furthermore contain an interval within S5 with a conspicuous return to heavier $\delta^{18}O_{G.\ ruber\ (w)}$ values that has no significant corresponding equivalent in the SST records. Using a depositional period for S5 of 4–5 kyr [21,22], the duration of this interval amounts to 700–900 yr.

As discussed above, the abundance profiles for *G. scitula* (Figs. 2e and 3) show a conspicuous peak (> 15%) followed by an abrupt drop to total absence (event 8 in Fig. 2a–c; labelled as f4 in [21]) in all three cores. In core KS205 and Hole 971A, these features coincide with the core and termination of the $\delta^{18}O_{G.\ ruber\ (w)}$ anomaly, respectively (Fig. 2a,b). The directly corresponding interval of Hole 967C shows no sign of this isotope anomaly (Fig. 2c). The record for Hole 967C was validated by a second series of 42 independently sampled, picked, and analysed $\delta^{18}O_{G.\ ruber\ (w)}$ points through S5, which fully confirmed the absence of the isotope anomaly. The presence in 967C of both the *G. scitula* abundance peak and its subsequent sharp drop to zero prior to the gap (Fig. 2e) proves that the reconstructed ~4.5-cm hiatus shown in Fig. 2c [21] postdates the level where the $\delta^{18}O_{G.\ ruber\ (w)}$ anomaly should be expected. We contend therefore that the $\delta^{18}O_{G.\ ruber\ (w)}$ record of Hole 967C, located close to the Nile outflow, displays a genuinely different behaviour in this respect than the $\delta^{18}O_{G.\ ruber\ (w)}$ records for the more westerly locations of KS205 and Hole 971A. It is also relevant that the lightest overall $\delta^{18}O_{G.\ ruber\ (w)}$ values occur at Site 971. This corroborates observations of a $\delta^{18}O$ minimum in the same area, separate from the Nile

←

Fig. 3. Summary overview after [21]. Plots of several of the main isotopic and faunal records through S5 in the three sites investigated, versus the 971A equivalent depth scale. For breakdown of the 'warm species' groupings, see [21]. Note the high degree of agreement in overall signal structures as well as detailed alignments.

impact, as made first for Holocene sapropel S1 [33] and recently confirmed for the majority of Quaternary sapropels [34].

In summary, therefore, the questions to be addressed concern: (1) the general excess depletion in $\delta^{18}O_{G.\ ruber\ (w)}$ typical for S5 that is not explicable by SST change; (2) the fact that a concentration of lightest $\delta^{18}O_{G.\ ruber\ (w)}$ values within S5, and other sapropels, is found between Libya and Southwest Crete; and (3) the return to heavier $\delta^{18}O_{G.\ ruber\ (w)}$ values in the westerly sites, and the absence of this event in the easterly site near the Nile outflow, again not related to SST.

The first issue of excess $\delta^{18}O$ depletions is well understood; there is a close association between sapropel occurrence and precession-driven northern hemisphere insolation maxima, and there is a link between sapropel deposition in the eastern Mediterranean and decreased deep-water ventilation due to enhanced freshwater flooding from intensified African summer monsoons [17,18,35–38]. The monsoon precipitation was characterised by $\delta^{18}O$ compositions as light as -6 to $-12‰$, as measured in aquifer waters and palaeo-lake carbonates [39–42], and its discharge into the Mediterranean Sea caused distinct $\delta^{18}O$ shifts to reduced values in foraminiferal species such as *G. ruber* (w) that live close to the surface during the monsoon season (i.e. late summer) [29].

Within this context of astronomical (precession) control, the issue concerning the location of the lightest $\delta^{18}O_{G.\ ruber\ (w)}$ values can be addressed. Traditionally, the Nile River was considered the dominant route for the excess monsoon discharge into the eastern Mediterranean at times of sapropel formation [17,18,35,43]. However, the observation that a concentration of lightest $\delta^{18}O_{G.\ ruber\ (w)}$ values occurs between Libya and Southwest Crete within a majority of Quaternary sapropels [33,34] including S5 (this study), suggests that monsoon flooding affected the eastern Mediterranean along much wider tracts of the North African margin (see also [44]). This would agree with the presence of vast fossil river systems, now buried beneath shifting sands, which constitute northward drainage routes from the central Saharan mountain ranges that were habitable monsoon-fed regions during (at least) the Holocene monsoon maximum [39,45] (Fig. 1). A striking image of such a major (>5 km wide) buried system at Kufra (23.3°N–22.9°E) was acquired by the SIR-C/X-SAR imaging radar aboard space shuttle Endeavour on October 4, 1994 [46]. We infer that the observed concentrations of lightest $\delta^{18}O_{G.\ ruber\ (w)}$ values between Libya and Southwest Crete reflect (re-)activation of these fossil river systems during the Eemian, as part of a pervasive mechanism that – based on previous observations [33,34] – operated during many Quaternary monsoon maxima.

Direct monsoon drainage from the wider North African margin depends on sufficient northward penetration of the Intertropical Convergence Zone (ITCZ) over the African continent to cross the main watershed at roughly 21°N (Fig. 1) [45,47,48]. Intensive northward penetration would be facilitated by vegetation-related reduction of the Saharan albedo, as proposed previously for the 'green Sahara' phase of the Holocene monsoon maximum [49,50]. Here, it should be emphasised that the pronounced seasonal migration of the ITCZ over the African continent [39] would constrain any 'western' monsoon flux from the 'Libyan' Basin (Fig. 1) to only one/two summer months of maximum northward ITCZ displacement. The fact that such discharge would cause a distinct region of concentrated very light $\delta^{18}O_{G.\ ruber\ (w)}$ values within the eastern Mediterranean is suggestive of rapid (wadi-type?) flood discharge that allowed only limited en-route evaporation to alter the isotopic signal of the highly convective (light $\delta^{18}O$) precipitation of the ITCZ.

Within this context, the distinct mid-sapropel return to heavier $\delta^{18}O_{G.\ ruber\ (w)}$ values in our western cores, and its absence in the eastern site, can be addressed (Fig. 2). The inferred western monsoon flux would be very sensitive to any relaxation of the maximum northward ITCZ penetration. In contrast, the channelling of monsoon-fed runoff via the Nile does not share this on/off sensitivity, since the vast Nile catchment (Fig. 1) [47,48] includes tropical to monsoon-affected latitudes irrespective of the extent of ITCZ penetration – it does so even today, during a monsoon minimum period. We therefore infer that the east-

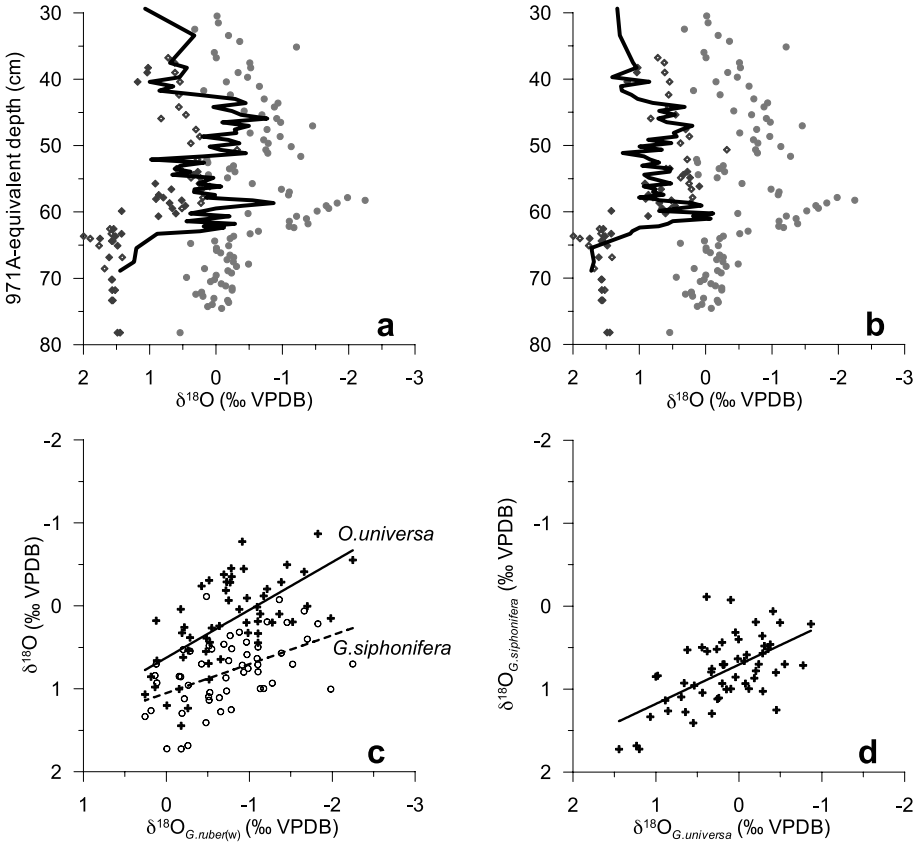

Fig. 4. Multi-species $\delta^{18}O$ results for S5 in core KS205. (a) Comparison of the $\delta^{18}O$ record of *O. universa* (black line) with the data for *G. ruber* (w) in solid dots, *N. pachyderma* (d) in open diamonds, and *G. scitula* in solid diamonds. (b) Same as (a), but using *G. siphonifera* (black line) instead of *O. universa*. (c) Correlations between $\delta^{18}O_{G.\ ruber\ (w)}$ and $\delta^{18}O_{O.\ universa}$, and between $\delta^{18}O_{G.\ ruber\ (w)}$ and $\delta^{18}O_{G.\ siphonifera}$. Statistics of the fits: $N=55$; $R^2=0.41$; $\delta^{18}O_{Ou}=0.58\ \delta^{18}O_{Gr}+0.63$ and $N=55$, $R^2=0.23$, $\delta^{18}O_{Gsi}=0.35\ \delta^{18}O_{Gr}+1.05$. (d) Correlation between $\delta^{18}O_{O.\ universa}$ and $\delta^{18}O_{G.\ siphonifera}$. Fit statistics: $N=57$, $R^2=0.35$, $\delta^{18}O_{Gsi}=0.47\ \delta^{18}O_{Ou}+0.71$.

ern Site 967 recorded the Nile's integrated signal of overall monsoon intensification, while the western sites reflect the much more sensitive 'western' system of direct drainage from the wider North African margin that became interrupted for 7–9 centuries in response to a relaxation in the northward penetration of the ITCZ.

4.2. Testing the hypothesis

We now evaluate the above working hypothesis against potential alternative explanations for the isotopic contrasts through S5.

One possibility would be that the alkenone SST record predominantly reflects winter temperature (hence the close correspondence with the $\delta^{18}O_{G.\ scitula}$ and $\delta^{18}O_{N.\ pachyderma\ (d)}$ records, both from species that thrive below the thermocline in winter-type waters), while the light 'anomalies' in $\delta^{18}O_{G.\ ruber\ (w)}$ reflect anomalously high summer temperatures. To explain the variability in the up to 2.0–2.5‰ contrasts between $\delta^{18}O_{G.\ ruber\ (w)}$ and $\delta^{18}O_{G.\ scitula}$ or $\delta^{18}O_{N.\ pachyderma\ (d)}$, however, such an hypothesis would require fluctuations of up to ~10°C in the summer–winter SST contrast. This seems highly unlikely in a basin where the present-day mean seasonal SST contrast amounts to only ~6°C [51]. Moreover, this option can be excluded by comparing the $\delta^{18}O_{G.\ ruber\ (w)}$ series with the $\delta^{18}O$ record of *Orbulina universa* (Fig.

4a), another summer mixed-layer dweller [29,30]. Although the $\delta^{18}O_{O.\ universa}$ series shows variability similar to $\delta^{18}O_{G.\ ruber\ (w)}$, it reaches only about half the amplitude (Fig. 4a,c). The implication is that $\delta^{18}O_{G.\ ruber\ (w)}$ and $\delta^{18}O_{O.\ universa}$ likely responded to the same environmental forcing, but that some sort of differentiation took place in the signal amplitudes within the summer mixed layer. This differentiation (up to 1‰ in $\delta^{18}O$) would imply the presence of a rather unrealistic temperature gradient of the order of 4°C within the summer mixed layer.

A far more realistic case can be made within the context of the freshwater-related working hypothesis presented above. It considers the isotopic compositions of the various species as the result of a mixing line between freshwater input and open marine water. We propose that significant freshwater influxes disturbed the summer mixed layer, and that either: (1) *G. ruber* (w) was more tolerant to this impact than *O. universa*, in agreement with observations in the Caribbean that *G. ruber* dominates in reduced-salinity lenses caused by freshwater discharge from the Orinoco River [52]; or (2) *G. ruber* (w) was simply more affected by freshwater dilution because it occupies a shallower habitat than *O. universa*. In either case, the effects on the isotope contrast between *G. ruber* (w) and *O. universa* would be the same: *G. ruber* (w) experiences the most dramatic $\delta^{18}O$ shifts since it records the freshwater impact in its most concentrated form, while *O. universa* records a signal that results from the mixing of this impact through the more voluminous summer mixed layer (which dampens the amplitude of the 'imported' $\delta^{18}O$ anomaly).

The applicability of the 'mixing-line' concept can be evaluated by considering results from another species analysed here, *G. siphonifera* (Fig. 4b). Although not tightly constrained, this species appears to be typical of winter conditions [29], in which case its $\delta^{18}O$ variability would be expected to approach that in $\delta^{18}O_{G.\ scitula}$ and $\delta^{18}O_{N.\ pachyderma\ (d)}$. Indeed, $\delta^{18}O_{G.\ siphonifera}$ values are generally heavy and show relatively low intra-S5 variability, marking it as a species with strong isotopic affinity to the winter-type conditions recorded also by *G. scitula* and *N. pachyderma* (Fig. 4b). When considered in detail, however, $\delta^{18}O_{G.\ siphonifera}$ appears considerably more variable than $\delta^{18}O_{G.\ scitula}$ and $\delta^{18}O_{N.\ pachyderma\ (d)}$. In fact, $\delta^{18}O_{G.\ siphonifera}$ differs from the latter two in that it still exhibits significant positive correlations with both $\delta^{18}O_{G.\ ruber\ (w)}$ and $\delta^{18}O_{O.\ universa}$ (Fig. 4c,d). We note that the amplitude of response to the environmental (freshwater) forcing that was roughly halved from $\delta^{18}O_{G.\ ruber\ (w)}$ to $\delta^{18}O_{O.\ universa}$ appears to be roughly halved again for $\delta^{18}O_{G.\ siphonifera}$. Overall, the isotope results agree with modern habitat observations [29] in that they place *G. siphonifera* in the winter mixed layer. This water mass, reflecting winter conditions, is roughly twice as deep/voluminous as the summer mixed layer, and so reflects an even further diluted expression of the summer-time freshwater-related $\delta^{18}O$ anomaly.

Finally, the subsurface winter-water dwellers *G. scitula* and *N. pachyderma* (d) record roughly similar absolute values to *G. siphonifera*, but with even less variability. These species by preference reside in deep subsurface habitats within a water mass that represents a long-term average mixing product of winter waters. Deep subsurface habitat preferences have been previously inferred [53] and observed [54] for *N. pachyderma* (d) in the Mediterranean, and for *G. scitula* in general [30].

One further potential counter-hypothesis needs to be considered: could the strong shifts in $\delta^{18}O_{G.\ ruber\ (w)}$ relative to the other species perhaps reflect habitat shifting? In this scenario, the strong depletions in $\delta^{18}O_{G.\ ruber\ (w)}$ might be explained in the same way as above, as the result of freshwater discharge, but there would not have been an 'interruption' in the monsoon maximum. Instead, the relapse to heavy $\delta^{18}O_{G.\ ruber\ (w)}$ values in the middle of S5 in core KS205 and Hole 971A would be considered the result of a shift in the main habitat of *G. ruber* (w) out of the freshwater-influenced surface conditions, perhaps because salinities became too low. Conceivably, *G. ruber* (w) would then have shifted to niches within the greater summer mixed layer, similar to *O. universa*. In essence, this scenario assumes that the enriched interval represents the peak of monsoon freshwater discharge, causing such low salinities that *G. ruber* (w) abandons its surface habitat.

This scenario, however, is hard to reconcile with the fact that similar trends to those in $\delta^{18}O_{G.\ ruber\ (w)}$ are observed in $\delta^{18}O_{O.\ universa}$ and $\delta^{18}O_{G.\ siphonifera}$, since a culmination of monsoon discharge would cause isotope depletions also throughout the summer and winter mixed layers. Hence, $\delta^{18}O_{O.\ universa}$ and $\delta^{18}O_{G.\ siphonifera}$ should then shift to reduced values, while *G. ruber* would show a unique, opposite, isotope shift due to its habitat shift. This counter-hypothesis is incompatible with the observations.

The failure of either counter-hypothesis to satisfactorily explain the data offers strong support to the feasibility of our working hypothesis of Eemian monsoon variability, which we may now assess within a wider geographic and temporal context.

4.3. A wider perspective

Using a likely approximation of 124–119 ka BP for the period of deposition of S5 [22], the approximate timing and duration of the reconstructed monsoon disruption within S5 (122.5–121.4 ka BP) closely resembles that estimated for an Eemian fluctuation found in a Northeast Mediterranean (Northwest Greece) vegetation record, with a drop in both summer and winter temperatures between ~121 and ~120.4 ka BP [55]. It further resembles the timing of a cooling event in data from central France [56] and Lake Baikal [57]. Current dating technology cannot resolve whether or not these Eemian events were coeval between the widely spaced sites, but we note a striking similarity to a spatially (virtually) synchronous climatic event observed around 8 ka BP in well-dated Holocene records.

Eastern Mediterranean sapropel S1, formed during the Early Holocene monsoon maximum (~9–6 ka BP), shows a comparable 'relapse' (~8 ka BP) to that reported here for Eemian S5. The event within sapropel S1 even culminated in a 500–600-yr interruption of the characteristic anoxic/dysoxic sea-floor conditions [9,58,59]. During the Holocene monsoon maximum, North Africa suffered basically similar climatic (ITCZ) variability to that inferred here for the Eemian, as witnessed by variations in – for example – North African lake levels [39], wind-blown dust fluxes into the Atlantic Ocean [60] and a range of sedimentological and archaeological indicators for humidy in the Fezzan (Southwest Libya) [61]. The ~8-ka-BP 'relapse' within sapropel S1 correlates with a weakening in the African monsoon intensity/penetration, with an especially harmful return of severe aridity near the northern limit of ITCZ penetration (at that time up to 18 or even 22°N) [39]. At the same time, the S1 'relapse' documents intensified impact of harsh higher-latitude climate conditions on the Mediterranean region [62], with intensification in the frequency/intensity of cold northerly air outbreaks over the basin in relation to enhanced (winter) Siberian High pressure conditions [9].

For the Eemian case, the combined data also seem to suggest a widespread cooling event, affecting (at least) France [56], Greece [55], and Siberia [57], with concomitant relaxation in the northward penetration of the African monsoon (this study). We further note that the inferred expression of centennial- to millennial-scale climate variability, in terms of concomitant relative dominance shifts between monsoonal and high-latitude circulation in mid latitudes, is not unique. It has also been recognised in variability during the last glacial cycle: the warmer Dansgaard–Oeschger (D–O) interstadials show signs of intensified monsoons (e.g. [1,63]) and weakened high-latitude circulation [2], while cold D–O stadials show the opposite (synthesis in [8]).

Since our interpretation involves large-scale climatic systems, it needs emphasis that the reported intra-Eemian event appears roughly coeval to sharp anomalies observed outside the Mediterranean region, in Atlantic and Indo–Pacific records. ODP Site 1059A (Blake Outer Ridge) in the subtropical western North Atlantic shows a heavy anomaly in $\delta^{18}O_{G.\ ruber}$ within MIS 5e (Eemian) around 123–121 ka BP that reaches the equivalent of ~2°C cooling [64], while ODP Site 769 in the Sulu Sea – i.e. in the 'western Pacific warm pool' – shows a remarkably similar heavy $\delta^{18}O_{G.\ ruber}$ anomaly around 122–121 ka BP (also equivalent to ~2°C cooling) [65]. Some fossil reef records suggest a corresponding minor sea-level drop (e.g. Huon Peninsula [66,67], Northwest Red Sea

[68]), but its absence in other studies [69,70] questions a truly eustatic nature.

5. Concluding remarks

A pervasive mechanism appears to underlie the centennial- to millennial-scale climate variability through glacial as well as interglacial times. This is not a new result [11,12], but the nature of the mechanism has remained elusive to date. The present paper argues, from new data on the Eemian and in reference to previous studies of the last glacial cycle and the Holocene, that a fundamental anti-phase relationship is consistently involved between monsoon penetration and the intensity of higher-latitude circulation in the northern hemisphere.

The tropical to subtropical latitudes receive the vast bulk of solar energy [63]. If solar variability is involved in driving the climate variability [2,9,10,12,71,72], therefore, the best chance of detecting the climate response is in sensitive regions near critical boundaries of the primary systems that transport the (solar) energy to higher latitudes. The atmospheric Hadley cells, their seasonal latitudinal displacements, and the cross-equatorial air flows associated with monsoon circulation, are crucial to both the heat transport from the low to mid latitudes and inter-hemispheric energy transfer. Monsoon penetration studies such as the present offer evidence of latitudinal Hadley cell displacements, which modelling studies suggest to be sensitive indicators of a climate response to solar variability [73]. Furthermore, the present study highlights the need for a deeper understanding of the interactions between monsoons and high-latitude climate within the centennial- to millennial-scale variability.

Acknowledgements

We thank J. Thomson for stimulating discussions. Data and calibration information are available from the authors: fauna and stable isotopes (E.Rohling@soc.soton.ac.uk), organic geochemistry of cores 971A and 967C (kay.emeis@iowarnemuende.de), and organic geochemistry of core KS205 (ibou@ccr.jussieu.fr). We thank C. Hemleben (chief scientist) and our other colleagues on the 12 November–11 December M51-3 cruise of R.V. *Meteor* in the eastern Mediterranean for interesting discussions. ***[BARD]***

References

[1] H. Schultz, U. VonRad, H. Erlenkeuser, Correlation between Arabian Sea and Greenland climate oscillations of the past 110,000 years, Nature 393 (1998) 54–57.
[2] P.A. Mayewski, L.D. Meeker, M.S. Twickler, S. Whitlow, Q. Yang, M. Prentice, Major features and forcing of high latitude northern hemisphere atmospheric circulation using a 110,000-year-long glaciochemical series, J. Geophys. Res. 102 (1997) 26345–26366.
[3] T. Blunier, J. Chapellaz, J. Schwander, A. Dällenbach, B. Stauffer, T.F. Stocker, D. Raynaud, J. Jouzel, H.B. Clausen, C.U. Hammer, S.J. Johnsen, Asynchrony of Antarctic and Greenland climate change during the last glacial period, Nature 394 (1998) 739–743.
[4] W. Dansgaard, S.J. Johnsen, H.B. Clausen, D. Dahl-Jensen, N.S. Gundestrup, C.U. Hammer, C.S. Hvidberg, J.P. Steffensen, A.E. Sveinbjornsdottir, J. Jouzel, G. Bond, Evidence for general instability of past climate from a 250 kyr ice core, Nature 364 (1993) 218–219.
[5] P.M. Grootes, M. Stuiver, J.W.C. White, S. Johnsen, J. Jouzel, Comparison of oxygen isotope records from the GISP2 and GRIP Greenland ice cores, Nature 366 (1993) 552–554.
[6] W.S. Broecker, Abrupt climate change: causal constraints provided by the paleoclimate record, Earth-Sci. Rev. 51 (2000) 137–154.
[7] M. Sarnthein, J.P. Kennett, J. Chappell, et al., Exploring Late Pleistocene climate variations, EOS Trans., Am. Geophys. Union, 81 (2000) 625 and 629–630.
[8] E.J. Rohling, P.A. Mayewski, P. Challenor, On the timing and mechanism of millennial-scale climate variability during the last glacial cycle, Clim. Dyn., in press.
[9] E.J. Rohling, P.A. Mayewski, A. Hayes, R.H. Abu-Zied, J.S.L. Casford, Holocene atmosphere–ocean interactions: records from Greenland and the Aegean Sea, Clim. Dyn. 18 (2002) 587–593.
[10] S.R. O'Brien, P.A. Mayewski, L.D. Meeker, D.A. Meese, M.S. Twickler, S.I. Whitlow, Complexity of Holocene climate as reconstructed from a Greenland ice core, Science 270 (1995) 1962–1964.
[11] G. Bond, W. Showers, M. Cheseby, R. Lotti, P. Almasi, P. deMenocal, P. Priore, H. Cullen, I. Hajdas, G. Bonani, A pervasive millennial-scale cycle in North Atlantic Holocene and Glacial climates, Science 278 (1997) 1257–1266.
[12] G. Bond, B. Kromer, J. Beer, R. Muscheler, M.N. Evans,

W. Showers, S. Hoffmann, R. Lotti-Bond, I. Hajdas, G. Bonani, Persistent solar influence on north Atlantic climate during the Holocene, Science 294 (2001) 2130–2136.
[13] N.J. Shackleton, Oxygen isotopes, ice volume and sea level, Quat. Sci. Rev. 6 (1987) 183–190.
[14] E. Bard, C. Jouannic, B. Hamelin, P. Pirazzoli, M. Arnold, G. Faure, P. Sumosusastro, Syaefudin, Pleistocene sea levels and tectonic uplift based on dating of corals from Sumba Island, Indonesia, Geophys. Res. Lett. 23 (1996) 1473–1476.
[15] J. Jouzel, C. Lorius, J.R. Petit, C. Genthon, N.I. Barkov, V.M. Kotlyakov, V.M. Petrov, Vostok Ice Core – A continuous isotope temperature record over the last climatic cycle (160,000 Years), Nature 329 (1987) 403–408.
[16] J. Guiot, A. Pons, J.L. deBeaulieu, M. Reille, A 140,000-Year continental climate reconstruction from 2 European pollen records, Nature 338 (1989) 309–313.
[17] M. Rossignol-Strick, African monsoons, an immediate climate response to orbital insolation, Nature 304 (1983) 46–49.
[18] M. Rossignol-Strick, Palaeogeogr. Palaeoclimatol. Palaeoecol. 49 (1985) 237–263.
[19] COHMAP members. Climatic changes of the last 18,000 years observations and model simulations. Science 241 (1988) 1043–1052
[20] J. Chappellaz, E. Brook, T. Blunier, B. Malaizé, CH_4 and $\delta^{18}O$ of O_2 records from Antarctic and Greenland ice: A clue for stratigraphic disturbance in the bottom part of the Greenland Ice Core Project and the Greenland Ice Sheet Project 2 ice cores, J. Geophys. Res. 102 (1997) 26547–26557.
[21] T. Cane, E.J. Rohling, A.E.S. Kemp, S. Cooke, R.B. Pearce, High-resolution stratigraphic framework for Mediterranean sapropel S5: defining temporal relationships between records of Eemian climate variability, Palaeogeogr. Palaeoclimatol. Palaeoecol. 183 (2002) 87–101.
[22] M. Bar-Matthews, A. Ayalon, A. Kaufman, Timing and hydrological conditions of Sapropel events in the Eastern Mediterranean, as evident from speleothems, Soreq cave, Israel, Chem. Geol. 169 (2000) 145–156.
[23] K.-C. Emeis, H.-M. Schulz, U. Struck, T. Sakamoto, H. Doose, H. Erlenkeuser, M. Howell, D. Kroon, M. Paterne, Stable isotope and temperature records of sapropels from ODP Sites 964 and 967: Constraining the physical environment of sapropel formation in the Eastern Mediterranean Sea, in: A.H.F. Robertson, K.-C. Emeis, C. Richter and A. Camerlenghi (Eds.), Proc. ODP, Sci. Res. 160 Ocean Drilling Program, College Station, TX, 1998, pp. 309–331.
[24] A. Rosell-Melé, E. Bard, K.-C. Emeis, J.O. Grimalt, P. Müller, R. Schneider, I. Bouloubassi, B. Epstein, K. Fahl, A. Fluegge, K. Freeman, M. Goni, U. Gütner, D. Hartz, S. Hellebust, T. Herbert, M. Ikehara, R. Ishiwatari, K. Kawamura, F. Kenig, J. de Leeuw, S. Lehman, L. Mejanelle, N. Ohkouchi, R.D. Pancost, C. Pelejero, F. Prahl, J. Quinn, J.-F. Rontani, F. Rostek, J. Rullkötter, J. Sachs, T. Blanz, K. Sawada, D. Schulz-Bull, E. Sikes, C. Sonzoni, Y. Ternois, G. Versteegh, J. Volkman, S. Wakeham, Precision of the current methods to measure the proxy UK'37 and absolute abundance in sediments: Results of an inter-laboratory comparison study. Geochem. Geophys. Geosyst. (G3) 2 (2001) paper number 2000GC000141.
[25] P.J. Müller, G. Kirst, G. Ruhland, I. vonStorch, A. Rosell-Mélé, Calibration of the alkenone paleotemperature index UK'37 based on core tops from the eastern South Atlantic and the global ocean (60°N–60°S), Geochim. Cosmochim. Acta 62 (001) (1998) 1757–1772.
[26] K.-C. Emeis, U. Struck, H.-M. Schulz, S. Bernasconi, T. Sakamoto, F. Martinez-Ruiz, Temperature and salinity of Mediterranean Sea surface waters over the last 16,000 years: Constraints on the physical environment of S1 sapropel formation based on stable oxygen isotopes and alkenone unsaturation ratios, Palaeogeogr. Palaeoclimatol. Palaeoecol. 158 (2000) 259–280.
[27] I. Cacho, J.O. Grimalt, M. Canals, Response of the western Mediterranean Sea to rapid climatic variability during the last 50,000 years: a molecular biomarker approach, J. Mar. Sys. 33–34 (2002) 253–272.
[28] Y. Ternois, M.-A. Sicre, A. Boireau, M.H. Conte, G. Eglinton, Evaluation of long-chain alkenones as paleotemperature indicators in the Mediterranean Sea, Deep-Sea Res. I 44 (1997) 271–286.
[29] C. Pujol, C. Vergnaud-Grazzini, Distribution patterns of live planktic foraminifers as related to regional hydrography and productive systems of the Mediterranean Sea, Mar. Micropaleontol. 25 (1995) 187–217.
[30] Ch. Hemleben, M. Spindler, O.R. Anderson, Modern Planktonic Foraminifera, Springer, New York, 1989, 363 pp.
[31] J.R. O'Neil, R.N. Clayton, T.K. Mayeda, Oxygen isotope fractionation on divalent metal carbonates, J. Chem. Phys. 51 (1969) 5547–5558.
[32] S.T. Kim, J.R. O'Neil, Equilibrium and nonequilibrium oxygen isotope effects in synthetic calcites, Geochim. Cosmochim. Acta 61 (1997) 3461–3475.
[33] M. Fontugne, M. Arnold, L. Labeyrie, M. Paterne, S. Calvert, J.-C. Duplessy, Paleoenvironment, sapropel chronology, and Nile river discharge during the last 20,000 years as indicated by deep-sea sediment records in the eastern Mediterranean, Radiocarbon 34 (1994) 75–88.
[34] K.-C. Emeis, H. Schulz, U. Struck, M. Rossignol-Strick, H. Erlenkeuser, M.W. Howell, D. Kroon, H. Mackensen, S. Ishizuka, T. Oba, T. Sakamoto, I. Koizumi, Eastern Mediterranean surface water temperatures and $\delta^{18}O$ composition during deposition of sapropels in the late Quaternary, Paleoceanography, in press.
[35] M. Rossignol-Strick, V. Nesteroff, P. Olive, C. Vergnaud-Grazzini, After the deluge; Mediterranean stagnation and sapropel formation, Nature 295 (1982) 105–110.
[36] P.G. Myers, K. Haines, E.J. Rohling, Modelling the paleo-circulation of the Mediterranean: The last glacial maximum and the Holocene with emphasis on the formation of sapropel S1, Paleoceanography 13 (1998) 586–606.

[37] E.J. Rohling, S. DeRijk, The Holocene Climate Optimum and Last Glacial Maximum in the Mediterranean: the marine oxygen isotope record, Mar. Geol. 153 (1999) 57–75.
[38] E.J. Rohling, S. DeRijk, P.G. Myers, K. Haines, Palaeoceanography and numerical modelling: The Mediterranean Sea at times of sapropel formation, Geol. Soc. London Spec. Publ. 181, 2000, pp. 135–149.
[39] F. Gasse, Hydrological changes in the African tropics since the last glacial maximum, Quat. Sci. Rev. 19 (2000) 189–211.
[40] P. Hoelzmann, H.J. Kruse, F. Rottinger, Precipitation estimates for the eastern Saharan palaeomonsoon based on a water balance model of the West Nubian Palaeolake Basin, Glob. Planet. Ch. 26 (2000) 105–120.
[41] K. Rozanski, Deuterium and oxygen-18 in European groundwaters – links to atmospheric circulation in the past, Chem. Geol. (Isot. Geosc. Sect.) 52 (1985) 349–363.
[42] . J.A. McKenzie, Pluvial conditions in the eastern Sahara following the penultimate deglaciation: implications for changes in atmospheric circulation patterns with global warming, Palaeogeogr. Palaeoclimatol. Palaeoecol. 103 (1993) 95–105.
[43] D.A. Adamson, F. Gasse, F.A. Street, M.A.J. Williams, Late Quaternary history of the Nile, Nature 288 (1980) 50–55.
[44] H.J. Pachur, G. Braun, The paleoclimate of the central Sahara, Libya and the Libyan Desert, Palaeoecol. Afr. 12 (1980) 351–363.
[45] H.J. Pachur, Holozäne Klimawechsel in den nördlichen Subtropen, Nova Acta Leopoldina NF88 331 (2001) 109–131.
[46] Wadi Kufra Radar Image http://southport.jpl.nasa.gov/imagemaps/html/srl-wadik.html (visited 5-10-2001), Image P-45719, 1995.
[47] C. Revenga, S. Murray, J. Abramovitz, A. Hammond, Watersheds of the World: Ecological Value and Vulnerability, World Resources Institute, Washington, DC, 1998, 200 pp.
[48] B.M. Fekete, C.J. Vörösmarty, W. Grabs, Global Composite Runoff Fields Based on Observed River Discharge and Simulated Water Balances, http://www.grdc.sr.unh.edu/html/paper/ReportA4.pdf (visited 11-06-2002), 2000, 115 pp.
[49] M. Claussen, V. Brovkin, A. Ganopolski, C. Kubatski, V. Petoukhov, Modelling global terrestrial vegetation–climate interaction, Phil. Trans. Roy. Soc. London 353 (1998) 53–63.
[50] V. Brovkin, M. Claussen, V. Petoukhov, A. Ganopolski, On the stability of the atmosphere–vegetation system in the Sahara/Sahel region, J. Geophys. Res. 103 (1998) 31613–31624.
[51] E.V. Stanev, H.J. Friedrich, S.V. Botev, On the seasonal response of intermediate and deep water to surface forcing in the Mediterranean Sea, Oceanol. Acta 12 (1989) 141–149.
[52] B. Schmucker, R. Schiebel, Planktic foraminifers and hydrography of the eastern and northern Caribbean Sea, Mar. Micropaleontol. (2002) in press.
[53] E.J. Rohling, W.W.C. Gieskes, Late Quaternary changes in Mediterranean Intermediate Water density and formation rate, Paleoceanography 4 (1989) 531–545.
[54] E.J. Rohling, M. DenDulk, C. Pujol, C. Vergnaud-Grazzini, Abrupt hydrographic change in the Alboran Sea (western Mediterranean) around 8000 yrs BP, Deep-Sea Res. 42 (1995) 1609–1619.
[55] M.R. Frogley, P.C. Tzedakis, T.H.E. Heaton, Climate variability in Northwest Greece during the last interglacial, Science 285 (1999) 1886–1889.
[56] N. Thouveny, J.-L. deBeaulieu, E. Bonifay, K.M. Creer, J. Guiot, M. Icole, S. Johnsen, J. Jouzel, M. Reille, T. Williams, D. Williamson, Climate variations in Europe over the past 140 kyr deduced from rock magnetism, Naure 371 (1994) 503–506.
[57] E. Karabanov, A.A. Prokopenko, D.F. Williams, G.K. Kursevich, Evidence for mid-Eemian cooling in continental climatic record from Lake Baikal, J. Paleolimnol. 23 (2000) 365–371.
[58] E.J. Rohling, F.J. Jorissen, H.C. DeStigter, 200 Year interruption of Holocene sapropel formation in the Adriatic Sea, J. Micropal. 16 (1997) 97–108.
[59] D. Mercone, J. Thomson, R.H. Abu-Zied, I.W. Croudace, E.J. Rohling, High-resolution geochemical and micropalaeontological profiling of the most recent eastern Mediterranean sapropel, Mar. Geol. 177 (2001) 25–44.
[60] P. deMenocal, J. Ortiz, T. Guilderson, J. Adkins, M. Sarnthein, L. Baker, M. Yarusinsky, Abrupt onset and termination of the African Humid Period: rapid climate responses to gradual insolation forcing, Quat. Sci. Rev. 19 (2000) 347–361.
[61] M. Cremaschi, Late Pleistocene and Holocene climatic changes in the central Sahara; the case study of the southwestern Fezzan, Libya, in: F.A. Hassan (Ed.), Droughts, Food and Culture – Ecological Change and Food Security in Africa's Later Prehistory, Kluwer/Plenum, New York, 2002, pp. 65–81.
[62] M. Rossignol-Strick, Sea–land correlation of pollen records in the eastern Mediterranean for the glacial–interglacial transition: biostratigraphy versus radiometric timescale, Quat. Sci. Rev. 14 (1995) 893–915.
[63] F. Sirocko, D. Leuschner, M. Staubwasser, J. Maley, L. Heusser, High-frequency oscillations of the last 70,000 years in the tropical/subtropical and polar climates, in: P.U. Clark, R.S. Webb, L.D. Keigwin (Eds.), Mechanisms of Global Climate Change at Millennial Time Scales, AGU Geophys. Monogr. 112, American Geophysical Union, Washington, DC, 1999, pp. 113–126.
[64] D.W. Oppo, L.D. Keigwin, J.F. McManus, J.L. Cullen, Persistent suborbital climate variability in marine isotope stage 5 and Termination II, Paleoceanography 16 (2001) 280–292.
[65] B.K. Linsley, Oxygen-isotope record of sea level and climate variations in the Sulu Sea over the past 150,000 years, Nature 380 (1996) 234–237.

[66] J. Chappell, N.J. Shackleton, Oxygen isotopes and sea level, Nature 324 (1986) 137–140.
[67] J. Chappell, A. Omura, T. Esat, M. McCulloch, J. Pandolfi, Y. Ota, B. Pillans, Reconciliation of late Quaternary sea levels derived from coral terraces at Huon Peninsula with deep sea oxygen isotope records, Earth Planet. Sci. Lett. 141 (1996) 227–236.
[68] J.C. Plaziat, J.L. Reyss, A. Choukri, F. Orszag-Sperber, F. Baltzer, B.H. Purser, Mise en évidence, sur la côte récifale d'Egypte, d'une régression interrompant brièvement le plus haut niveau du Dernier Interglaciaire (5e): un nouvel indice de variations glacio-eustatiques à haute fréquence au Pléistocène?, Bull. Soc. Géol. France 169 (1998) 115–125.
[69] M.T. McCulloch, T. Esat, The coral record of last interglacial sea levels and sea surface temperatures, Chem. Geol. 169 (2000) 107–129.
[70] P. Blanchon, A. Eisenhower, Multi-stage reef development on Barbados during the Last Interglaciation, Quat. Sci. Rev. 20 (2001) 1093–1112.
[71] B. van Geel, O.M. Raspopov, H. Renssen, J. van der Plicht, V.A. Dergachev, H.A.J. Meijer, The role of solar forcing upon climate change, Quat. Sci. Rev. 18 (1999) 331–338.
[72] J. Beer, W. Mende, R. Stellmacher, The role of the sun in climate forcing, Quat. Sci. Rev. 19 (2000) 403–415.
[73] J.D. Haigh, The impact of solar variability on climate, Science 272 (1996) 981–984.